Plant Soil (2023) 488:533–549
https://doi.org/10.1007/s11104-023-05991-y

RESEARCH ARTICLE

Tree stem and soil methane and nitrous oxide fluxes, but not carbon dioxide fluxes, switch sign along a topographic gradient in a tropical forest

Warren Daniel · Clément Stahl · Benoît Burban · Jean-Yves Goret · Jocelyn Cazal · Andreas Richter · Ivan A. Janssens · Laëtitia M. Bréchet

Received: 28 May 2022 / Accepted: 13 March 2023 / Published online: 9 May 2023

Abstract

Purpose Tropical forests exchange large amounts of greenhouse gases (GHGs: carbon dioxide, CO_2; methane, CH_4; and nitrous oxide, N_2O) with the atmosphere. Forest soils and stems can be either sources or sinks for CH_4 and N_2O, but little is known about what determines the sign and magnitude of these fluxes. Here, we aimed to study how stem and soil GHG fluxes vary along a topographic gradient in a tropical forest.

Methods Fluxes of GHG from 56 individual tree stems and adjacent soils were measured with manual static chambers. The topographic gradient was characterized by a soil moisture gradient, with one end in a wetland area ("seasonally flooded"; SF), the other end in an upland area ("terra firme"; TF) and in between a transitional area on the slope (SL).

Results Tree stems and soils were always sources of CO_2 with higher fluxes in SF compared to TF and SL. Fluxes of CH_4 and N_2O were more variable, even within one habitat. Results showed that, in TF, soils acted as sinks for N_2O whereas, in SF and SL, they acted as sources. In contrast, tree stems which were predominantly sources of N_2O in SF and TF, were sinks in SL. In the soil, N_2O fluxes were significantly influenced by both temperature and soil water content, whereas CH_4 fluxes were only significantly correlated with soil water content.

Conclusion SF areas were major sources of the three gases, whereas SL and TF soils and tree stems acted as either sources or sinks for CH_4 and N_2O. Our results indicate that tree stems represent overlooked sources of CH_4 and N_2O in tropical forests that need to be further studied to refine GHG budgets.

Keywords Greenhouse gas (GHG) exchange · Sink · Spatial variation · Soil · Source · Stem

Responsible Editor: Paul Bodelier.

Supplementary Information The online version contains supplementary material available at https://doi.org/10.1007/s11104-023-05991-y.

W. Daniel (✉) · I. A. Janssens · L. M. Bréchet
Center of Excellence Global Change Ecology, Department of Biology, University of Antwerp, Universiteitsplein 1, B-2610 Wilrijk, Belgium
e-mail: warren.daniel@uantwerpen.be

W. Daniel · C. Stahl · B. Burban · J.-Y. Goret · J. Cazal · L. M. Bréchet
INRAE, UMR EcoFoG, CNRS, CIRAD, AgroParisTech, Université des Antilles, Université de Guyane, 97310 Kourou, France

A. Richter
Centre for Microbiology and Environmental Systems Science, University of Vienna, Djerassiplatz 1, 1030 Wien, Austria

L. M. Bréchet
Department of Ecology and Evolutionary Biology, University of Arizona, Tucson, AZ, USA

Introduction

Tropical forests are a major component of the global carbon cycle (Mitchard 2018), mainly because they store half the world's forest biomass carbon (Pan et al. 2011) and represent about half of the global terrestrial carbon sink, taking up about 15% of the anthropogenic carbon emissions annually (Phillips and Brienen 2017). As part of the climate system, ecosystem uptake or emissions of carbon dioxide (CO_2), methane (CH_4) and nitrous oxide (N_2O) can mitigate or exacerbate global warming (Butterbach-Bahl et al. 2004). Fluxes of these greenhouse gases (GHGs) naturally occur in tropical forests but their quantification, origins and environmental controls still need to be determined. Studying soil and stem GHG fluxes along natural topographic transects is relevant because these transects cover large gradients in soil texture, water content and nutrient availability (Van Langenhove et al. 2021) and also exhibit differences in standing biomass and tree productivity (Ferry et al. 2010). This large range of soil properties along a topographic gradient is likely to influence GHG fluxes from soils and stems.

Soil CO_2 fluxes, resulting from both root and microbial activity, can be affected either directly by soil temperature, water content, nutrients and dissolved organic matter (Fang et al. 2009; Whitaker et al. 2014; Auffret et al. 2016), or indirectly by changes in soil texture and vegetation (Luizão et al. 2004; Epron et al. 2006; Bréchet et al. 2009), and hence vary with topographic position. High soil water content under warm temperatures can stimulate soil CO_2 efflux (Sorz and Hietz 2006; Barba et al. 2016), and, by promoting sap flux and stem respiration, also increase stem CO_2 efflux (Ceschia et al. 2002).

In stems, CO_2 may indeed be produced locally during the respiration required to sustain production of new woody tissues (i.e. growth respiration) and maintenance of living biomass (i.e. maintenance respiration; Ryan 1990; Maier 2001). The latter often explains the differences in respiration rate between small and large trees (Ryan and Waring 1992), as well as the size-related changes in the efficiency of stem carbon accumulation. Stem CO_2 fluxes depend on tree height (Cavaleri et al. 2006; Katayama et al. 2014, 2016), season (Stahl et al. 2011) and elevation (Robertson et al. 2010), but not on bark thickness (Paine et al. 2010). In addition to the locally produced CO_2, stem CO_2 fluxes can also originate from respiration in the soil, where CO_2 dissolved in water can be taken up by the roots and transported with the xylem sap through the stem (Saveyn et al. 2008; Teskey et al. 2008; Trumbore et al. 2013; Hilman and Angert 2016; Aubrey and Teskey 2021). A fraction of this CO_2 can be fixed by photosynthetic cells in the wood or leaves (Teskey et al. 2008), whereas the rest will be emitted to the atmosphere and contribute to stem, branch and leaf CO_2 fluxes. The CO_2 emitted from stems thus originates from CO_2 produced in both the woody tissue and soil (Teskey et al. 2017). Soil water extremes, such as flooding or drought, can reduce stem CO_2 fluxes because they tend to reduce aerobic respiratory activity in soils (Stahl et al. 2011). Both stem and soil CO_2 fluxes show seasonal patterns explained by interactions between temperature, soil water content and sap flow (e.g. Barba et al. 2019). Soil water content can inhibit the transverse transport of CO_2 in trees, which correspond to the movement of CO_2 from leaves to stem and roots for use in cellular respiration and other metabolic processes. Water is essential for the vertical movement of dissolved nutrients and gases in trees, including CO_2. When soil water content is low, the water potential gradient between the soil and the roots decreases, making it more difficult for water and dissolved gases to move from the roots to the leaves (Sancho-Knapik et al. 2022). This can lead to a reduction in photosynthesis and transpiration, which can in turn reduce the CO_2 emissions from the stems (Zhao et al. 2018).

Topography is characterized by a hydrological and nutrient gradient (from well-drained upland areas ("terra firme"; TF) with aerobic conditions to waterlogged wetland areas ("seasonally flooded"; SF) with anaerobic conditions (Ferry et al. 2010; Courtois et al. 2018). To gain more insight in the variation of CO_2 fluxes across a tropical forest, the impact of topographic position on soil and stem CO_2 fluxes needs to be studied.

Methane can both be emitted and taken-up by soils and stems. Soil CH_4 uptake dominates in aerobic soils, such as the upland TF areas in tropical forests, and is generally a minor component of the forest GHG balance. Nonetheless, CH_4 uptake is an important flux in the global budget of atmospheric CH_4

since global aerobic soil surface is large (Dutaur and Verchot 2007; Saunois et al. 2020). In contrast, anaerobic soils, such as the SF areas in tropical forests, mainly emit CH_4, because methanogenesis dominates over aerobic microbial methanotrophy.

Recent studies have demonstrated that also tree stems can be a source of CH_4 (Pangala et al. 2013, 2017; Barba et al. 2019; Covey and Megonigal 2019; Epron et al. 2022). Tree stem CH_4 emissions are currently unaccounted for as an emission compartment in the current global CH_4 budget (Carmichael et al. 2014; Saunois et al. 2020). Moreover, several recent studies suggest that tree stem CH_4 fluxes may occur across a range of ecosystems including mangroves (Jeffrey et al. 2019, 2020), wetland forests (Pangala et al. 2017; Terazawa et al. 2015; Sjögersten et al. 2020; Gauci et al. 2022), while even upland forests may emit CH_4 (Covey et al. 2012; Machacova et al. 2016; Barba et al. 2019; Bréchet et al. 2021). These studies have demonstrated that tree stems can emit CH_4 even if they grow on soils that consume CH_4, and also that the drivers of spatial patterns and magnitudes of these fluxes remain poorly understood. Gauci et al. (2022) pinpointed a clear positive effect of water table on flooded-tree CH_4 emissions. In trees, a large fraction of the emitted CH_4 originates from CH_4 production in anaerobic soil layers, where CH_4 production exceeds CH_4 consumption (Welch et al. 2019; Feng et al. 2022). The gas dissolved in the soil water is taken up and transported by the roots, thereby bypassing the soil's uppermost aerobic layer where methanotrophy dominates (Megonigal and Guenther 2008). In addition to CH_4 delivered by the xylem stream, CH_4 can moreover be produced in the woody tissues by methanogenic archaeal communities decomposing the heartwood of trees (Yip et al. 2019). Low oxygen concentrations in woody tissues can create a suitable environment for methanogenic communities, enhancing their activity and abundance. Along a topographic gradient, trees in a specific local environment (TF or SF) can have specific water and oxygen contents, as well as specific methanogenic archaeal communities. By extension, it can be assumed that the origin and the amount of CH_4 emissions in stems are species-specific.

As for CO_2, in temperate forest the seasonal pattern in stem CH_4 fluxes has been explained by temperature, soil water content and tree sap flow (Maier et al. 2018; Barba et al. 2019; Welch et al. 2019; Machacova et al. 2021). An increase in stem CH_4 emissions can be correlated to an increase in soil and air temperature (Wang et al. 2016; Pitz et al. 2018; Barba et al. 2019), an increase in soil water content (Barba et al. 2019; Welch et al. 2019), or a decrease in water table depth (Pitz et al. 2018). In our study, we will examine the relationships between CH_4 fluxes in stems and soil along a topographic gradient associated with different habitats and microenvironment conditions (Pitz et al. 2018; Barba et al. 2019). In order to understand the processes involved in the emission and consumption of CH_4 in forest ecosystems, it is necessary to study the woody tissue biogeochemistry and anatomy and tree physiology (Covey and Megonigal 2019). Stem CH_4 emissions are indeed correlated with physiological or anatomical and morphological properties of tree species (Wang et al. 2016; Warner et al. 2017; Sjögersten et al. 2020), such as wood density (Wang et al. 2016), wood structure (Sjögersten et al. 2020), tree diameter (Pitz et al. 2018) and sap flow rate (Barba et al. 2019; Pitz and Megonigal 2017).

In soils, N_2O is naturally produced in a wide range of nitrogen turnover processes, mainly by nitrification and denitrification processes (Davidson et al. 2007). Nitrification is an oxidative process, dominating in aerated soils. In aerobic soils, such as the TF areas in forests, consumption of N_2O typically exceeds production of N_2O, thereby exhibiting lower N_2O emissions and even N_2O uptake. However, nitrate leaching into lower anaerobic soil layers may be denitrified, causing N_2O production and emission. Under the same anaerobic conditions where methanogenesis dominates, denitrification indeed dominates (Davidson et al. 2000). Denitrification by many bacterial and fungal taxa not only produces N_2O; under anoxic conditions, N_2O can be further reduced to N_2, thus yielding lower N_2O emissions (Smith et al. 2003). In ecosystems exhibiting variation in soil water, spatial and temporal variation in N_2O emissions and uptake is thus extremely high, depending on variation in nitrate production and in N_2O production and consumption. As the water-filled pore space decreases and the concentration of oxygen rises, the aerobic metabolism of bacteria, archaea and fungi can outcompete the anaerobic metabolism, lowering the rate of N_2O emission and increasing the probability for net N_2O emissions.

In trees, N_2O dissolved in soil water can be absorbed by the roots and transported with the transpiration stream (Machacova et al. 2013). The role of

trees in forest N_2O budgets has been largely overlooked (but see: Machacova et al. 2016; Wen et al. 2017; Welch et al. 2019). Studies on mature trees growing in natural field conditions are limited and have revealed notable N_2O emissions from stems (Díaz-Pinés et al. 2016; Machacova et al. 2016). In boreal forest, a study revealed that stem N_2O fluxes can be linked to the tree's physiological activity, such as gross primary productivity and evapotranspiration (Machacova et al. 2019). In temperate forest, stem N_2O emissions in upland trees occurred even without aerenchyma (a specific plant tissue facilitating gas exchange along stems), and were associated with the rates of xylem water transport (Díaz-Pinés et al. 2016). Stem N_2O emissions might be a pathway of N_2O produced in the soil and emitted from terrestrial ecosystems into the atmosphere. As for stem CH_4 fluxes, an increase in stem N_2O fluxes is expected with an increase in soil water content along a topographic gradient.

The simultaneous study of fluxes of these three GHGs from or into soils and stems may yield new insights on the complexity of forest ecosystems as sources and sinks of GHGs. The overall goal of this study was to characterize the spatial variation of CO_2, CH_4 and N_2O fluxes and, more specifically, examine the effect of topography-driven variation in abiotic conditions on these fluxes in a tropical forest, in French Guiana. We hypothesized that 1) GHG fluxes measured on tree stems across a topographic transect show similar trends to those on soils, 2) abiotic factors such as soil temperature and soil water content that are known to control CO_2, CH_4 and N_2O fluxes in soil, also drive fluxes in tree stems, and 3) tree properties that determine the conductivity of the GHGs, such as bark and sapwood density or bark thickness, co-determine the GHG fluxes from stems.

Materials and methods

Study site

The experiment was conducted at the Paracou research station (5°50'N, 52°55'W), located in the coastal area of French Guiana, South America. Paracou is a pristine tropical forest with an average tree density of 620 trees ha^{-1} and a tree species richness between 150 and 200 species ha^{-1}, both for trees with diameter at breast height (1.30 m; DBH) > 10 cm. The Lecythidaceae, Fabaceae, Sapotaceae and Chrysobalanaceae families are the dominant plant families in this highly diverse forest (Gourlet-Fleury et al. 2004). The study site is characterized by a patchwork of hills (10 - 40 m a.s.l.) and soils are mostly nutrient-poor Acrisols (FAO / ISRIC / ISSS 1998) with pockets of sandy Ultisols. Soils developed over a Precambrian metamorphic formation, called the "Bonidoro series", are composed of schist and sandstone with veins of pegmatite, aplite, and quartz (Bonal et al. 2008). Annual rainfall at the study site (2004 - 2015) averages 3100 ± 70 mm $year^{-1}$ and mean annual air temperature is about 25.7 ± 0.1 °C (Aguilos et al. 2019). The north-south movement of the intertropical convergence zone strongly influences the precipitation regime and makes the tropical climate very seasonal. The wet season can last eight months (December - July) and alternates with a dry period of about four months (August - November) during which rainfall is generally less than 100 mm $month^{-1}$.

Sampling design

The campaign was carried out in February 2020, i.e. during the wet season. The selection of the trees was based on a precise representation of the distribution of diameter classes in the experimental plots (Supplementary, Fig. S6). The experimental plots were in the footprint of the Guyaflux tower (Bonal et al. 2008). We selected three topographic positions along the topographic transect: 1) terra firme located on top of hills (TF), 2) slopes at intermediate elevation (SL) and 3) seasonally flooded at low elevation very close to the water of the permanent river (SF). These different topographic positions were characterized by differences in volumetric soil water content (mean values measured during the campaign: 0.17 ± 0.02 m^3 m^{-3} in TF, 0.23 ± 0.02 m^3 m^{-3} in SL and 0.46 ± 0.14 m^3 m^{-3} in SF), but also in a suite of other environmental characteristics (Table 1). In this study, TF was present at the highest elevation level and its soils were typically characterized by a high clay content, water drainage, and organic matter content but a low pH. SF occurred at the lowest elevation and had soils with high water contents and bulk density but low root biomass and carbon content, likely due to the lower clay content (Soong et al. 2020). These soils experienced at least three consecutive months of flooding during the year (usually during the major rainy season between April and July; Ferry et al. 2010). Between TF and SF, SL

Table 1 Vegetation and soil characteristics of each topographic position, i.e. TF (terra firme), SL (slope) and SF (seasonally flooded), in the Paracou tropical forest, French Guiana. Stand density included every tree with a diameter > 10 cm DBH. Bark and sapwood density were calculated as dry mass / green volume / ρ water. Bark and sapwood water content were taken the week following the flux campaign and were calculated as ((humid mass - dry mass) / dry mass) × 100

Topographic position	SF	SL	TF
Stand structure			
Altitude (m)	12.81 ± 0.72	21.04 ± 2.43	27.43 ± 1.51
Stand density (stem ha^{-1})	565	520	606
Basal area (m^2 ha^{-1})	30.80	26.98	31.96
Species / ha	193	202	208
Surface (ha)	3.51	5.46	3.04
Mean diameter (cm)	22.63 ± 13.98	22.13 ± 13.24	22.61 ± 13.21
Soil characteristics			
Soil type [x]	haplic gleysol	haplic acrisol	hypoferralic acrisol
Volumetric soil water content (m^3 m^{-3})	0.46 ± 0.14	0.23 ± 0.02	0.17 ± 0.02
Soil temperature (°C)	24.52 ± 0.13	24.54 ± 0.22	25.52 ± 0.61
Root density (g cm^{-3})[x]	2.72 ± 0.51	7.11 ± 1.33	7.23 ± 1.82
Clay content (%)	12	17	26
SOC (kg m^{-3})[x]	17.32 ± 3.41	24.01 ± 2.63	29.02 ± 2.44
pH[x]	4.38 ± 0.05	4.24 ± 0.03	4.21 ± 0.04
Stem characteristics			
Bark thickness (mm)	6.50 ± 4.15	5.11 ± 2.00	5.84 ± 3.01
Bark density (g cm^{-3})	0.53 ± 0.27	0.52 ± 0.09	0.51 ± 0.13
Sapwood density (g cm^{-3})	0.54 ± 0.14	0.65 ± 0.07	0.64 ± 0.12
Bark water content (%)	135.78 ± 66.15	120.33 ± 29.52	135.93 ± 81.95
Sapwood water content (%)	87.81 ± 34.97	71.93 ± 14.44	70.34 ± 19.24

[x]from Epron et al. (2006)

was characterized by transitional soils (Table 1). Soil types were hypoferralic acrisol on TF, haplic acrisol on SL, and haplic gleysol on SF according to Epron et al. (2006). Briefly, in Epron et al. (2006), six soil cores (3.3-cm diameter, 6.0-cm depth) were sampled for each topographic transect. Root fragments (< 5-mm diameter) were washed, oven-dried at 60 °C to constant mass and weighed. Soil pH was determined in a 1:2.5 soil:water ratio. The six soil subsamples of each plot were pooled into a composite sample. The concentrations of organic carbon were determined on these 30 composite samples with a total organic carbon analyser (TOC-5050- Shimadzu, Japan).

Forty-five polyvinylchloride (PVC) collars of 20 cm in diameter were inserted into the soil one year prior to the first measurement (December 2018) to an average depth of 3.0 cm (± 0.5 cm). For each topographic position, five circular plots of 5 m radius were identified by three PVC collars arranged 1 m apart to form a triangle (Fig. 1). The diameter measurements and botanical determination of the trees maximum 5 m around the collars were carried out during the same period. A total of 56 trees were selected (ranging from 2 to 7 trees per plot), given in total 20 trees in TF and 18 in both SL and SF.

Soil and stem fluxes

Gas samples were taken with manual static chambers and a syringe. We took gas samples once per individual tree, between February 2 and 4, 2020. For the soil CO_2, CH_4 and N_2O flux measurements, we used the PVC chambers described in Courtois et al. (2018) between 9 am and 3 pm to avoid diurnal variability (Bréchet et al. 2011; Courtois et al. 2018; Pavelka et al. 2018). Soil chambers'volume and surface area were 2600 cm^3 and 290 cm^2, respectively. The dimensions of tree stem chambers were 10.0 cm length, 8.0 cm width, 10.5 cm depth and 84.0 cm^2 surface area accounting for a total volume of 840 cm^3. Manual tree stem chambers were made with Tupperware boxes (LocknLock, Seoul, Korea), allowing us to fix them on all trees bigger than 12 cm diameter with straps and rubber Teroson (Henkel, Dusseldorf, Germany). We installed the stem chambers at 1.30 m above the soil surface. In total, 180 soil and 280 measurements of GHG concentration in the tree stems were made during the field campaign. Four gas concentration measurements per collar and per tree were taken to compute the GHG fluxes. We performed a single measure for each selected tree

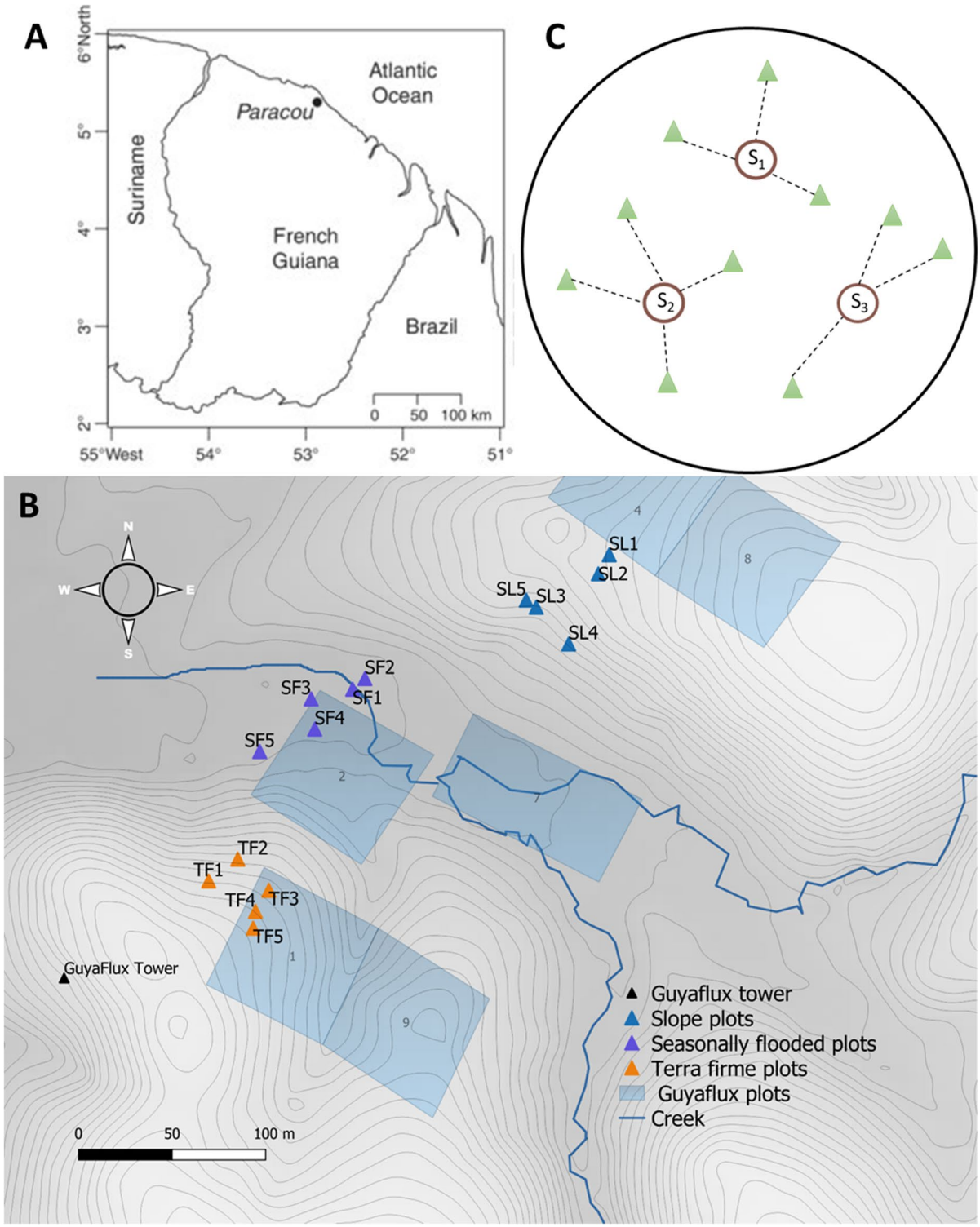
A
6°North
5°
4°
3°
2°
55°West
54°
53°
52°
51°
Atlantic Ocean
Paracou
Suriname
French Guiana
Brazil
0 50 100 km
C
S1
S2
S3
B
N
W
E
S
SL1
SL2
SL5
SL3
SL4
SF2
SF3
SF1
SF4
SF5
TF2
TF1
TF4
TF3
TF5
GuyaFlux Tower
4
8
2
7
1
9
0 50 100 m
Guyaflux tower
Slope plots
Seasonally flooded plots
Terra firme plots
Guyaflux plots
Creek

◂**Fig. 1** Site location and experimental design. **A** Location of the study site Paracou, French Guiana. **B** Location of the fifteen plots near six permanent plots belonging to the Guyaflux experimental tropical forest, in Paracou. Plots are symbolized by triangles; there were five plots in each habitat along the topographic gradient, such as orange triangles for terra firme (TF1-5), blue triangles for slope (SL1-5) and purple triangles for seasonally flooded (SF1-5). **C** Experimental setup plot, a circular plots of 5 m radius with three soil sampling points (collars S1, S2 and S3) and tree sampling triangle (N = 3 to 7 per collars)

in the three habitats during the wet season. During the sampling period, SF was indeed flooded with high soil water content (0.46 m^3 m^{-3}) in our wet season of measurements. Gas samples were extracted from chambers at 0, 10, 20 and 30 min for soil and tree stems. In the soil and stems, air samples were taken with a 15-mL syringe whose needle was inserted through a septum in the chamber and then injected into pre-evacuated 12-mL vials (Labco Limited, Ceredigion, UK). The chambers were not ventilated and after the first air sampling, the air inside the chamber headspace was mixed five times with the syringe prior sampling. For each sample, concentrations of CO_2, CH_4 and N_2O were determined by gas chromatography (Trace GC Ultra, Thermo Fisher Scientific, Vienna, Austria) and a vacuum dosing system (S + H Analytics, Germany) at 50 °C on a molecular sieve column (ShinCarbon ST 100 / 120, 2 m × 1 mm ID 1 / 16" OD, Restek). We used a flame ionization detector (FID) with a methanizer for CH_4 detection and a pulsed-discharge detector for N_2O detection. Calculation of minimum detectable flux (MDF) of CH_4 and N_2O was made with the methodology developed by Parkin et al. (2012). At sampling time 0, the mean concentration (that is, ambient concentration) were, for N_2O, 0.360 ppm and 0.380 ppm for the soil and stem, respectively, and for CH_4, 2.17 ppm and 2.22 ppm for the soil and stem, respectively. The soil CH_4 and N_2O MDF was 9.80 µgC m^{-2} h^{-1} and 13.06 µgN m^{-2} h^{-1}, implying that values of CH_4 fluxes within the range [−9.80; +9.80 µgN m^{-2} h^{-1}] were included in the analysis as null fluxes (idem for N_2O; Table S2 in Supplementary).

In addition, flux determination using manual chamber techniques in the soil and stems relied on discrete samples collected from a chamber headspace over fixed time intervals at 0, 10, 20 and 30 min. Flux computation were determined as the change in gas concentration over the time using linear or exponential curve fitting procedures.

Fluxes were computed with the "gasfluxes" package (version 0.4 - 4; Fuss 2020) for the three gases using linear regression (LR), or revised Hutchinson / Mosier (HMR) methods following recommendations from Pedersen et al. (2010) where HMR fluxes with the modified H / M technique from gas concentrations of each time interval (C_0, C_1, C_2, and C_3) as:

$$f_0 = \frac{\left(C_{A1,2} - C_0\right)^2}{\left[t_{A1,2} \times \left(2 \times C_{A1,2} - C_3 - C_0\right)\right]} \times \ln\left[\frac{\left(C_{A1,2} - C_0\right)}{\left(C_3 - C_{A1,2}\right)}\right] \quad (1)$$

where f_o is the calculated flux, C_0 is the headspace concentration at time 0, $C_{A1,2}$ is the average of the headspace concentrations at time C_1 and C_2, and C_3 is the chamber headspace gas concentration at time 3. The term "$t_{A1,2}$" is the time interval corresponding to the average of time 1 and time 2 (or one half of the total chamber deployment time). Gasfluxes provides functions for fitting non-linear concentration time models as well as convenience functions for checking data and combining different calculation methods. HMR is robust against horizontal gas transport and patterns of non-linearity, which reduces several constraints on static chamber methods, such as insertion depth and deployment time.

After flux computations, 62% of CO_2 fluxes were fitted with HMR methods and 38% with LR methods. For CH_4, 8% of the fluxes were estimated through LR methods whereas 92% were fitted with HMR methods and for N_2O, 17% of the fluxes were calculated with HMR methods and 83% with LR method. Gas mixing ratios (ppm) were converted using the ideal gas law to determine the amount of gas in headspace (on a mole or mass basis), normalized by the surface area of each static flux chamber. Fluxes of CO_2 passed all the above data cleaning steps. However, 27.7% of CH_4 fluxes (13.3% of soil CH_4 fluxes and 57% of stem CH_4 fluxes) and 54.4% of N_2O fluxes (31% of soil N_2O fluxes and 82% of stem N_2O fluxes) had to be removed because they did not exceed the detection limit (Parkin et al. 2012).

Soil and stem characteristics

Ancillary environmental variables were simultaneously measured in the soil and tree stems. Soil surface temperature and volumetric water content were

recorded at the same time than flux measurements. These measurements were taken at three locations around each collar using a digital waterproof thermometer at 10 cm depth (HI98501, Hanna instruments, UK) and a dielectric soil moisture sensor, with general mineral soil calibration, at 5 cm depth (SM150T, Delta-T Devices, UK). Data of root density, soil organic matter content and pH were from Epron et al. (2006) for the same three topographic positions. In addition, 56 wood samples were taken with a wood cutter of 40 mm in diameter and at DBH.

A 150-mm digital Vernier caliper (Mitutoyo Inc., Japan) was used to measure bark thickness of the wood samples. Wood water content of these samples was calculated with a balance (Sartorius Analytical Balance CPA224, Sartorius AG, Germany; precision = 1.10^{-4} g) to determine the fresh and dry mass before and after the samples were placed in the oven at 103 °C for 48 hours. Bark and sapwood density of the same samples were the dry biomass in a unit of volume of green wood.

Scaling up

Fluxes of CO_2, CH_4 and N_2O in the tree stems and soil beneath the same trees were scaled up to one hectare by habitat of the studied tropical forest using the stem diameter at DBH, surface area of the five circular plots of 5 m radius within each topographic position and tree basal area. Various challenges can limit the tree flux estimations. The process of extrapolation from plot measurements to regional scale assumes that these plots are representative of the region. Our scaling up was based on four important steps: 1) the three selected habitats were within the footprint of the Guyaflux tower (Fig. 1) and covered 29% (3.5 ha), 45% (5.46 ha) and 25% (3.04 ha) of the surface area for TF, SL and SF, respectively, 2) in each habitat, five circular plots were set up, and tree selection was based on the diameter class of the permanent plots of the Guyaflux unit (Fig. S5). Results of this selection were very closed to values of the natural distribution of the tree community. 3) Calculation of the total surface of the trees was based on the method developed by Chambers et al. (2004), and applied by Rowland et al. (2018), and 4) because of too heterogeneous results from previous studies (Plain et al. 2019; Katayama et al. 2021; Moldaschl et al. 2021; Epron et al. 2022), no vertical pattern was applied for the studied GHGs. The assumption for the stem area flux estimation was that there was a strong functional relationship between total stem surface area (SA) and DBH and total tree stem SA calculation was based on Chambers et al. (2004) equation (Eq. (2)).

$$SA = 10\hat{}\left(-0.105 - 0.686 \times \log_{10}(DBH) + 2.208 \times \log_{10}(DBH)^2 - 0.627 \times \log_{10}(DBH)^3\right) \quad (2)$$

where SA is the surface area in m^2 and DBH the diameter at breast height in cm. This scaling equation is based on simplified tree forms, and may not accurately represent the diversity of branching structures, which exists in tropical forests. This equation was used to estimate SA for each tree inside the five plots in each habitat. In total, the surface stem for 56 trees varied from 12.25 cm to 100 cm in diameter. Finally, for each habitat, SA was multiplied by the flux of each tree, and the sum of the total stem and soil flux per hectare of habitat was calculated.

For each circular plot, the estimated tree stem fluxes per gas were the sums of SA multiplied by the corresponding gas fluxes of each tree. To determine the exact soil surface area (SS; m^2) of each plot, the stem basal areas (m^2) were calculated and removed from the plot surface area, 78.5 m^2. For each circular plot, estimated soil fluxes were the sums of SS multiplied by the corresponding gas fluxes of each soil collar. Up scaled CO_2, CH_4 and N_2O fluxes from the tree stems and surrounding soils of each forested topographic position, i.e. SF, SL and TF, were then expressed in hectare of forest. The tree stem to soil ratios were calculated for each gas and each forested topographic position.

Statistical analyses

Shapiro - Wilk normality tests were used to determine whether the data were normally distributed ($p < 0.05$). We tested for differences in GHG fluxes between TF, SL and SF for fluxes of both soil and tree stems using Kruskal - Wallis One Way Analysis of Variance on Ranks. Dunn's Method was then used to pinpoint

which specific means are significantly different from the others ($p < 0.05$) using pairwise multiple comparison procedures. To obtain more representative GHG fluxes, we averaged the three GHG fluxes per plot ($N = 5$ for the soil; $2 < N < 7$ for tree stems). Data analyses, including descriptive statistics and data visualisation were conducted in the R statistical programming environment (v.3.6.3; R Core Team 2020).

Results

Soil and stem CO_2, CH_4 and N_2O fluxes

Despite a slightly more pronounced soil CO_2 emission in SF than in TF (146 ± 39 mgC m^{-2} h^{-1} and 124 ± 25 mgC m^{-2} h^{-1}, respectively), there were no significant differences between the three topographic positions regarding soil CO_2 fluxes. In contrast, topographic position had a significant effect (Kruskal - wallis, $p < 0.001$) on soil CH_4 and N_2O fluxes. The soil was a net emitter of CH_4 in SF (43 ± 149 µgC m^{-2} h^{-1}) and a CH_4 consumer in SL and TF (-13 ± 22 µgC m^{-2} h^{-1} and -110 ± 91 µgC m^{-2} h^{-1}, respectively). Soil CH_4 fluxes were significantly different between TF and SL ($p < 0.001$) and between TF and SF ($p < 0.01$). N_2O fluxes were very low compared with CO_2 fluxes. In SF and SL, soils were sources of N_2O with 14 ± 23 µgN m^{-2} h^{-1} and 11 ± 9 µgN m^{-2} h^{-1}, respectively. However, the soils in TF acted as sinks for N_2O (-15 ± 25 µgN m^{-2} h^{-1}). N_2O fluxes were significantly different between TF and SL ($p < 0.001$) and between TF and SF ($p < 0.05$; Fig. 2C).

Topographic position also significantly (Kruskal - wallis, $p < 0.001$) affected stem fluxes, albeit only for CO_2 and N_2O fluxes ($p < 0.001$). Tree stem CO_2 emissions were significantly higher in SF than in TF (55 ± 15 mgC m^{-2} h^{-1} and 35 ± 5 mgC m^{-2} h^{-1}, respectively, $p < 0.01$, Fig. 2D). Stems tended to be sources of CH_4 in SF (4 ± 9 µgC m^{-2} h^{-1}), but not in SL and TF (0 ± 2 µgC m^{-2} h^{-1} and 0 ± 11 µgC m^{-2} h^{-1}, respectively), but the topographic positions did not differ in stem CH_4 fluxes. In SL and TF, tree stems consumed N_2O (-31 ± 32 µgN m^{-2} h^{-1} and -4 ± 18 µgN m^{-2} h^{-1}, respectively), whereas tree stems emitted N_2O in SF (13 ± 13 µgN m^{-2} h^{-1}). There was a significant difference in N_2O fluxes between SL and SF ($p < 0.001$) and between SL and TF ($p < 0.01$).

While soils and stems exhibited fluxes of similar direction for CO_2 at all topographic positions, this was not the case for the other GHGs. In general, the direction of CH_4 fluxes in soils and tree stems was similar, with both acting as sources in SF but exhibiting opposite directions in TF and SL. Specifically, in SF, both soils and tree stems were sources of CH_4, while in TF and SL, soil was a sink of CH_4 and tree stems were a source of CH_4. Nonetheless, in all three habitats both positive and negative stem fluxes occurred. In agreement with CH_4 fluxes, SF showed emissions of N_2O, while TF showed consumptions of N_2O from both soils and stems. In SL, however, soil was a source, while tree stems were a sink of N_2O.

Soil and stem characteristics

There were significant differences in soil temperature and soil water content among the three topographic positions (Fig. 3). Soil temperature in TF was significantly higher from the other two topographic positions, while soil water content was significantly different among the three topographic positions. The correlation matrix (Table 2) indicated that soil CH_4 fluxes were positively correlated with soil water content and negatively correlated with soil temperature. A significant negative correlation ($p < 0.05$) was observed between soil temperature and soil N_2O flux. Surprisingly, in our study, none of the measured stem traits correlated significantly with the stem GHG fluxes.

Scaling up

For the tree stems, the up-scaled flux rates of CO_2, CH_4 and N_2O to the plot level in each topographic position ranged from 1238 to 1453 gC ha^{-1} h^{-1}, −67 to 122 mgC ha^{-1} h^{-1}, and −67 to −0.9 mgN ha^{-1} h^{-1}, respectively. Overall, tree stems were mainly a sink of N_2O in the three topographic positions, whereas they shifted from sinks to strong sources of CH_4 between TF and SF (Supplementary, Fig. S6). In TF, tree stems emitted the equivalent of 73% of the soil CO_2 emissions and of 6% and 55% of the soil CH_4 and N_2O consumptions (Supplementary, Fig. S7). In SF, stem fluxes were 85% of CO_2, 28% of CH_4 and −6% of N_2O, compared with soil GHG fluxes.

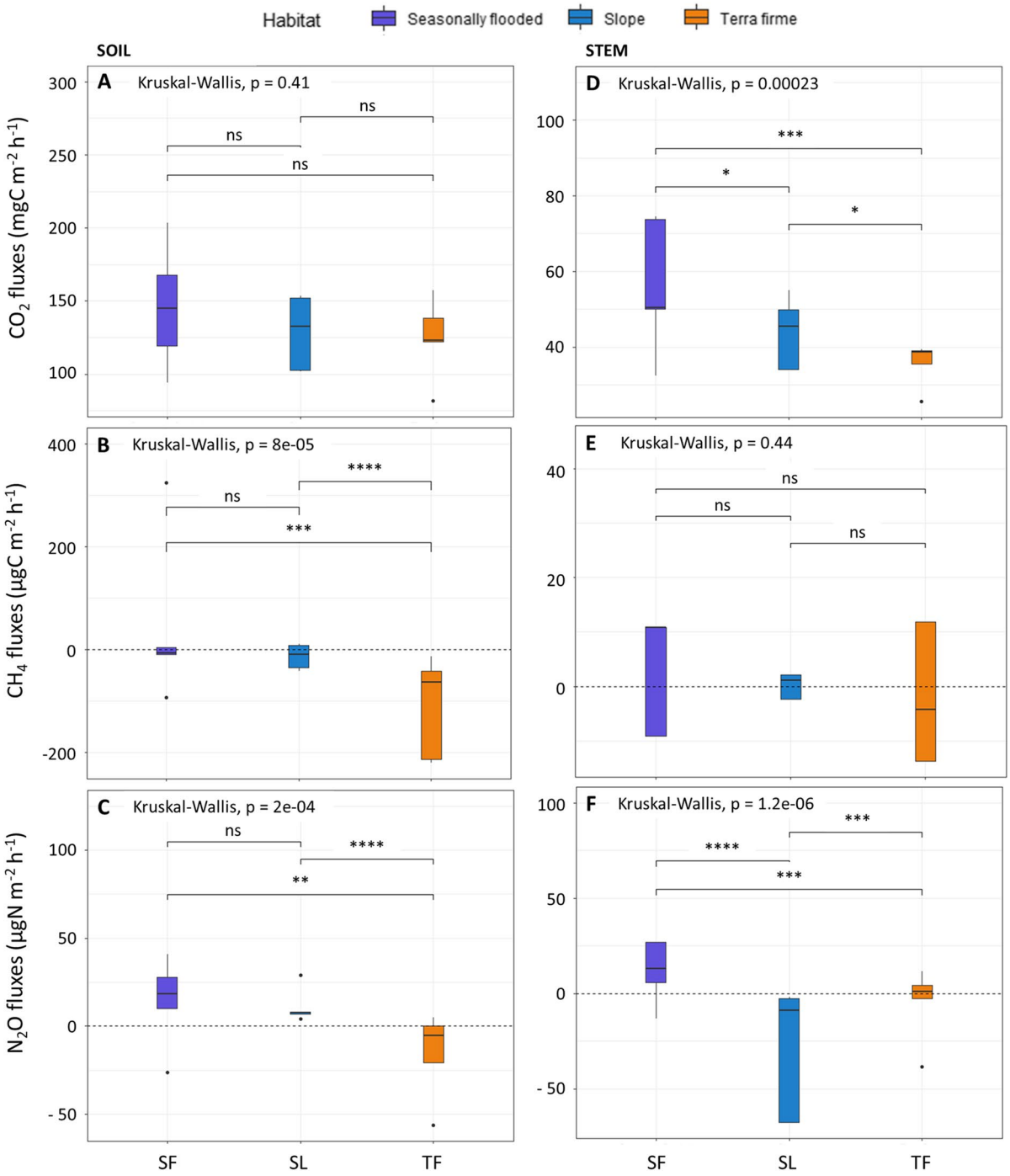

Fig. 2 Variation of soil and stem GHG fluxes in three topographic positions, i.e. SF (seasonally flooded; purple), SL (slopes; blue) and TF (terra firme; orange). Boxplot for **A** CO_2, **B** CH_4 and **C** N_2O are fluxes measured in the soil and **D** CO_2, **E** CH_4 and **F** N_2O are fluxes measured in the stems. Boxplots show the quartiles (box), median (horizontal bar), upper and lower extremes (whiskers) and outliers (dots) of all plots over the different stem and soil locations (N = 5). Stem fluxes were calculated per stem area. Asterisks indicate significant differences between soil and stem GHG fluxes in three topographic positions, with **** for $p <= 0.0001$, *** for $p <= 0.001$, ** for $p <= 0.01$, * for $p <= 0.05$ and ns for $p > 0.05$ when non-significant, based on Kruskal-Wallis statistical tests

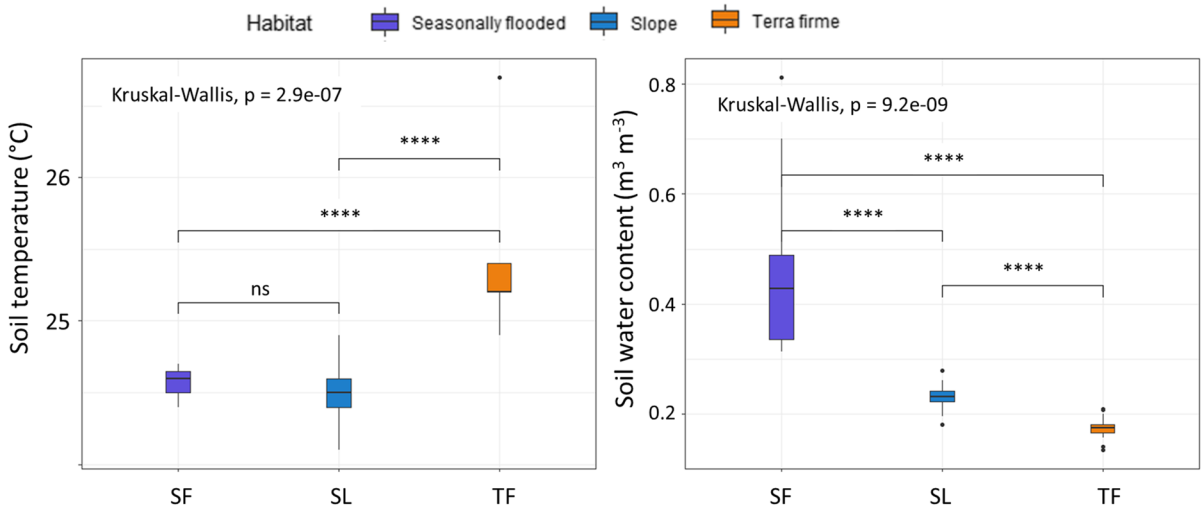

Fig. 3 Variation of soil temperature (°C) and soil water content (m^3 m^{-3}) between the three topographic positions, i.e. SF (seasonally flooded; purple), SL (slope; blue) and TF (terra firme; orange). Soil water content is expressed as volumetric water content. Asterisks indicate significant differences between soil temperature and soil water content in three topographic positions, with **** for $p <= 0.0001$, *** for $p <= 0.001$, ** for $p <= 0.01$, * for $p <= 0.05$ and ns for $p > 0.05$ when non-significant, based on Kruskal-Wallis statistical tests

Table 2 P value from Spearman's correlations between fluxes of CO_2, CH_4 and N_2O and the soil and stem variables

	Soil CO_2 flux	Soil CH_4 flux	Soil N_2O flux
Soil			
Soil temperature	0.597	**0.011**	**0.035**
Soil water content	0.474	**0.044**	0.226
	Stem CO_2 flux	Stem CH_4 flux	Stem N_2O flux
Stem			
Bark thickness	0.119	0.898	0.863
Bark density	0.062	0.145	0.970
Sapwood density	0.969	0.102	0.604
Bark water content	0.368	0.984	0.958
Sapwood water content	0.810	0.423	0.680

Values in bold indicate statistically significant correlations at the $p < 0.05$ level ($N = 15$)

Discussion

This study aimed at understanding whether soil and stem CO_2, CH_4 and N_2O fluxes responded similarly to the changes in environmental conditions across a topographic gradient, and at identifying controls of these fluxes.

Spatial topographic gradient does not affect CO_2 emissions

We observed that soil CO_2 fluxes did not differ among the three topographic positions, despite the difference in soil water content (factor 3 between SF and TF). Soil CO_2 fluxes (81 - 203 mgC m^{-2} h^{-1} or 0.51 - 1.28 µmol m^{-2} s^{-1}) were within the range of values previously reported for French Guianese forests during the wet season (Janssens et al. 1998; Bonal et al. 2008; Rowland et al. 2014; Courtois et al. 2018) or during the transition period between the wet and dry season (Epron et al. 2006; Bréchet et al. 2011). Other studies on the spatial variation in GHG fluxes in tropical forests also reported no effect of topographic position on soil CO_2 fluxes (Arias-Navarro et al. 2017; Courtois et al. 2018). The strong spatial heterogeneity in soil CO_2 fluxes might be due to the large diversity of tree species within each topographic position

(Table 1). Tree species can have a highly different chemical, structural and functional traits of roots and leaves, leading to contrasted litter types, which can influence biogeochemical and physical processes of decomposition related to microbial community activity and, hence, soil GHG fluxes (Townsend et al. 2008; Bréchet et al. 2011; Roland et al. 2013).

Tree stem CO_2 emissions on the other hand were significantly different in SF compared to SL and TF (Fig. 2). Stem CO_2 fluxes integrate processes of stem growth and stem maintenance respiration (Salomón et al. 2021, 2022), and flux rates depend on the diffusion rates as well as the internal CO_2 axial and radial transport (Teskey et al. 2008). According to Saveyn et al. (2008), the transport of respired CO_2 in xylem sap from roots to stems, especially under high sap flow rates, is not only a reflection of the rate of actual respiration of the living cells in the woody tissues. Several ecophysiological parameters as sap pH, stem temperature and gas diffusivity in the stem, which can change over time, are likely to have a significant impact on stem CO_2 fluxes (Teskey et al. 2008; Trumbore et al. 2013). In this study, we did not find any relationship with bark and wood traits, suggesting that stem CO_2 emissions were not necessarily limited by the thickness of the bark (Paine et al. 2010). At a larger scale, however, higher-density bark and sapwood tissues were shown to induce lower stem CO_2 fluxes for a given nitrogen mass than lower density tissues (Westerband et al. 2022), which underlines that multiple stem-traits affect their gas exchanges.

Spatial topographic gradient affects CH_4 fluxes

Contrary to previous studies (Wolf et al. 2012; Courtois et al. 2018), the topographic transect studied here did influence CH_4 fluxes, with soils in SF acting as sources, most likely due to low oxygen, and SL and TF as sinks, most likely due to more aerobic conditions (Table 1). In flooded soil, CH_4 is produced under anaerobic conditions (Jeffrey et al. 2020). Soil oxygen concentrations decline with an increase in soil water content, creating favourable conditions for methanogenesis. Concentrations of CH_4 in the soil rise, increasing dissolved CH_4 in soil water that is subsequently absorbed by tree roots and transported up to the stems.

Emissions of CH_4 in tree stems can dramatically increase the source strength of wetland forests and modestly decrease the sink strength of upland forests (Fig. 2E), offsetting the tropical forest carbon sink potential. In TF, aerobic conditions facilitate methanotrophic activity (Hanson and Hanson 1996; Maier et al. 2018; Welch 2018), explaining why CH_4 uptake was detected in the upper layer of the soils and the stem fluxes from TF (Table 1). Interestingly, CH_4 flux patterns were different between the soil and tree stems (Fig. 4). Some tree stems emitted CH_4, while the surrounding soil consumed CH_4, suggesting that there is a methanogenic microbial community specific to the tree (Feng et al. 2021) and / or that trees acted as a bypass of the upper soil layer in which all soil-produced CH_4 is oxidized. In our study, bark and sapwood traits had no effect on stem CH_4 fluxes, in agreement with results in Epron et al. (2022). Pangala et al. (2013) found that CH_4 fluxes in tropical tree stems were positively related to stem lenticel density, which was not measured in our study, suggesting that stem fluxes can be constrained by the features of the wood. Further studies are necessary to determine whether other traits such as the chemical composition and porosity of the wood can explain the variations in the stem GHG fluxes.

Spatial topographic gradient affects N_2O fluxes

Most of the soil N_2O fluxes measured in this study were emissions, except for TF where 75% of the fluxes were consumption. A possible explanation is that SL and SF soils were particularly humid and nitrogen-rich (Ferry et al. 2010). Previous results from other tropical soils showed similar trends concerning nitrogen-rich soil (Arias-Navarro et al. 2017). Nevertheless, soil water content was not linked with N_2O fluxes in our study site, as previously reported in Courtois et al. (2018). Several explanations can explain this lack of relationship. First, as the three topographic positions have different clay and sand contents (Epron et al. 2006), soil water content may also differ. Second, soil texture and soil water content at different depths can influence N_2O production, with drier soil layers at the surface than deeper in the soil (i.e. 5 cm). Third, N_2O can be produced under aerobic conditions by nitrification and can be denitrified to N_2, which was not measured in our study.

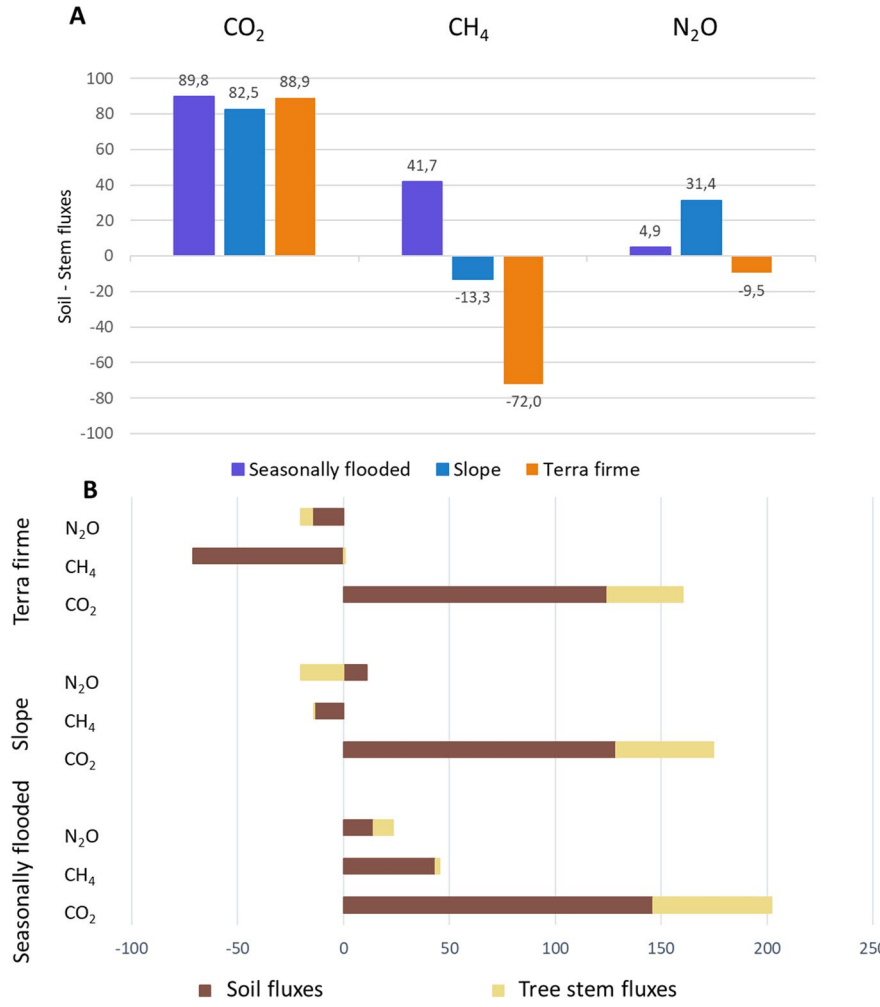

Fig. 4 **A** Difference between mean soil and mean stem GHG fluxes (mgC ha^{-1} h^{-1} for CO_2, µgC ha^{-1} h^{-1} for CH_4 and µgN ha^{-1} h^{-1} for N_2O) and **B** sum of mean soil and stem fluxes for each GHG flux and each topographic position (N = 5, number of plots per habitat)

Other soil properties such as total phosphorus and carbon to nitrogen ratio (Butterbach-Bahl et al. 2013) can influence the community composition of microorganisms, but these variables were not measured in our plots. There was no significant relationship between soil water content and N_2O emissions from tree stems in our study, which can be explained by the timing and frequency of measurements. In their studies, Machacova et al. (2013) demonstrated that stem N_2O emissions peaked 24 hours after rewetting, but then declined rapidly. It is therefore likely that the sampling periods did not always coincide with the maximum denitrification rates.

Scaling up

To our knowledge, flux measurements of simultaneously CO_2, CH_4 and N_2O in mature trees and soil of a highly diverse and heterogeneous tropical forest have never been reported, and it is only recently that trees are recognized as CH_4 and N_2O flux contributors (Warner et al. 2017; Maier et al. 2018; Welch 2018; Barba et al. 2019; Plain et al. 2019; Machacova et al. 2020; Schindler et al. 2020; Epron et al. 2022). Measuring flux from a single point on a tree stem and extrapolating it to the entire tree has already been described and used in the literature (Machacova et al. 2016; Warner et al. 2017). Indeed, results from tree

stem GHG flux studies are highly variable not always shown clear pattern across a vertical profile (Chambers et al. 2004; Epron et al. 2022; Katayama et al. 2014, 2021; Plain et al. 2019). In this study, we measured GHG flux at DBH and, while there are potential drawbacks to this extrapolation, such as oversimplification of flux upscaling, we believe it is a useful initial global approach.

In SF, where the flux differences were the highest, stems contributed up to 22% to total CH_4 emission (soil + stems) and in SL stems contributed up to 43% to total N_2O consumption. This showed that tropical tree stems cannot only emit carbon through CH_4 fluxes, but also take up a certain quantity of nitrogen from the atmosphere through N_2O fluxes. Nevertheless, interpretation of our scaling up approach should be made with caution due to the absence of repetitions over time, relatively small surface area (circular plots were 78 m^2, covering 393 m^2 of each forested topographic position) and rather simple allometric regression model for estimating the total tree stem surface area per plot. Since we carried out the flux measurements during the wet season, we assumed that the emissions of the stem CO_2, CH_4 and N_2O were not affected by lack of water into the soil, which can promote a decrease in the intensity of the transpiration stream and, hence, affect the transport of CH_4 and N_2O. In the soil, CO_2, CH_4 and N_2O fluxes are known to be highly heterogeneous due to highly variable physical, chemical and biological properties (Arias-Navarro et al. 2017; Courtois et al. 2018), whereas changes in stem CO_2, CH_4 and N_2O fluxes due to tree individuals and tree species traits remain poorly documented, especially for CH_4 and N_2O in tropical forest. Temporal variation in CO_2, CH_4 and N_2O fluxes in the stems and soils is also important to take into account when upscaling fluxes.

Conclusion

In the wet season conditions, our results not only revealed that tree stems accounted for non-negligible ecosystem GHG fluxes, but also that stems and the surrounding soils shifted from sinks to sources of CH_4 and N_2O along a topographic transect, while both remaining a source of CO_2. Soil CH_4 and N_2O fluxes differed among topographic positions with consistently higher CH_4 and N_2O fluxes in SF. Tree stem CO_2 and N_2O fluxes also differed among topographic positions, with higher CO_2 emission in SF and a pronounced stem N_2O consumption in SL. In our tropical forest site, temperature and soil water content were important environmental factors for soil N_2O fluxes, while soil water content was the main driver of soil CH_4 fluxes.

Being common in the Guiana shield and many other tropical areas, taking into account the effect of these topographic patterns can be relevant for modelling the tropical forest GHG budgets. The variation in CO_2, CH_4 and N_2O fluxes remained mostly unexplained, highlighting their high spatial and temporal variation. Despite the analysis of several wood traits, none of them explained the observed variations in stem CO_2, CH_4 and N_2O fluxes. Additional studies are thus required to disentangle the effect of the soil properties and tree stem traits on GHG fluxes. Future research in tropical forest is also necessary to determine which drivers control the temporal variations in tree stem GHG fluxes, knowing that intra-seasonal variations can influence the contributions of the trees to local and global GHG flux budgets.

Acknowledgements This work was supported by the European Research Council Synergy grant ERC-2013-SyG-610028-IMBALANCE-P, the European Commission through a Marie Skodowska-Curie Individual Fellowship H2020-MSCA-IF-2017-796438 to LMB, the Research Fund of the University of Antwerp and an "Investissement d'Avenir" grant delivered by the Agence Nationale de la Recherche (CEBA; ANR-10-LABX-25-01). We thank CIRAD - UMR EcoFoG for hosting our fieldwork.

References

Aguilos M, Stahl C, Burban B, Hérault B, Courtois E, Coste S et al (2019) Interannual and seasonal variations in ecosystem transpiration and water use efficiency in a tropical rainforest. Forests 10:14

Arias-Navarro C, Díaz-Pinés E, Klatt S, Brandt P, Rufino MC, Butterbach-Bahl K, Verchot LV (2017) Spatial variability of soil N_2O and CO_2 fluxes in different topographic positions in a tropical montane forest in Kenya. J Geophys Res: Biogeosci 122:514–527

Aubrey DP, Teskey RO (2021) Xylem transport of root-derived CO_2 caused a substantial underestimation of belowground respiration during a growing season. Glob Chang Biol 27(12):2991–3000

Auffret MD, Karhu K, Khachane A, Dungait JA, Fraser F, Hopkins DW et al (2016) The role of microbial community composition in controlling soil respiration responses to temperature. PLoS One 11:e0165448

Barba J, Curiel Yuste J, Poyatos R, Janssens IA, Lloret F (2016) Strong resilience of soil respiration components to

drought-induced die-off resulting in forest secondary succession. Oecologia 182:27–41
Barba J, Poyatos R, Vargas R (2019) Automated measurements of greenhouse gases fluxes from tree stems and soils: magnitudes, patterns and drivers. Sci Rep 9:1–13
Bonal D, Bosc A, Ponton S, Goret JY, Burban B, Gross P et al (2008) Impact of severe dry season on net ecosystem exchange in the Neotropical rainforest of French Guiana. Glob Chang Biol 14:1917–1933
Bréchet L, Ponton S, Roy J, Freycon V, Coûteaux MM, Bonal D, Epron D (2009) Do tree species characteristics influence soil respiration in tropical forests? A test based on 16 tree species planted in monospecific plots. Plant Soil 319:235–246
Bréchet L, Ponton S, Alméras T, Bonal D, Epron D (2011) Does spatial distribution of tree size account for spatial variation in soil respiration in a tropical forest? Plant Soil 347:293–303
Bréchet LM, Daniel W, Stahl C, Burban B, Goret JY, Salomón RL, Janssens IA (2021) Simultaneous tree stem and soil greenhouse gas (CO_2, CH_4, N_2O) flux measurements: a novel design for continuous monitoring towards improving flux estimates and temporal resolution. New Phytol 230:2487–2500
Butterbach-Bahl K, Kock M, Willibald G, Hewett B, Buhagiar S, Papen H, Kiese R (2004) Temporal variations of fluxes of NO, NO_2, N_2O, CO_2, and CH_4 in a tropical rain forest ecosystem. Global biogeochemical cycles
Butterbach-Bahl K, Baggs EM, Dannenmann M, Kiese R, Zechmeister-Boltenstern S (2013) Nitrous oxide emissions from soils: how well do we understand the processes and their controls? Philos Trans R Soc B: Biol Sci 368:20130122
Carmichael MJ, Bernhardt ES, Bräuer SL, Smith WK (2014) The role of vegetation in methane flux to the atmosphere: should vegetation be included as a distinct category in the global methane budget? Biogeochemistry 119:1–24
Cavaleri MA, Oberbauer SF, Ryan MG (2006) Wood CO_2 efflux in a primary tropical rain forest. Glob Chang Biol 12:2442–2458
Ceschia E, Damesin C, Lebaube S, Pontailler J-Y, Dufrene E (2002) Spatial and seasonal variations in stem respiration of beech trees (Fagus sylvatica). Ann For Sci 59:801–812
Chambers JQ, Tribuzy ES, Toledo LC, Crispim BF, Higuchi N, Santos JD et al (2004) Respiration from a tropical forest ecosystem: partitioning of sources and low carbon use efficiency. Ecol Appl 14:72–88
Courtois EA, Stahl C, Van den Berge J, Bréchet L, Van Langenhove L, Richter A, Urbina I, Soong JL, Penuelas J, Janssens IA (2018) Spatial variation of soil CO_2, CH_4 and N_2O fluxes across topographic positions in tropical forests of the Guiana shield. Ecosystems 21:1445–1458
Covey KR, Megonigal JP (2019) Methane production and emissions in trees and forests. New Phytol 222:35–51
Covey KR, Wood SA, Warren RJ, Lee X, Bradford MA (2012) Elevated methane concentrations in trees of an upland forest. Geophys Res Lett 39:1–6
Davidson EA, Keller M, Erickson HE, Verchot LV, Veldkamp E (2000) Testing a conceptual model of soil emissions of nitrous and nitric oxides: using two functions based on soil nitrogen availability and soil water content, the hole-in-the-pipe model characterizes a large fraction of the observed variation of nitric oxide and nitrous oxide emissions from soils. Bioscience 50:667–680
Davidson EA, de Carvalho CJR, Figueira AM, Ishida FY, Ometto JPH, Nardoto GB et al (2007) Recuperation of nitrogen cycling in Amazonian forests following agricultural abandonment. Nature 447:995–998
Díaz-Pinés E, Heras P, Gasche R, Rubio A, Rennenberg H, Butterbach-Bahl K, Kiese R (2016) Nitrous oxide emissions from stems of ash (Fraxinus angustifolia Vahl) and European beech (Fagus sylvatica L.). Plant Soil 398:35–45
Dutaur L, Verchot LV (2007) A global inventory of the soil CH_4 sink. Global Biogeochemical Cycles 21(4)
Epron D, Bosc A, Bonal D, Freycon V (2006) Spatial variation of soil respiration across a topographic gradient in a tropical rain forest in French Guiana. J Trop Ecol 22:565–574
Epron D, Mochidome T, Tanabe T, Dannoura M, Sakabe A (2022) Variability in stem methane emissions and Wood methane production of tree different species in a cold Temperate Mountain Forest. Ecosystems:1–16
Fang HJ, Yu GR, Cheng SL, Mo JM, Yan JH, Li S (2009) 13C abundance, water-soluble and microbial biomass carbon as potential indicators of soil organic carbon dynamics in subtropical forests at different successional stages and subject to different nitrogen loads. Plant Soil 320:243–254
Feng H, Guo J, Ma X, Han M, Kneeshaw D, Sun H, Wang W (2021) Methane emissions may be driven by hydrogenotrophic methanogens inhabiting the stem tissues of poplar. New Phytologist 233(1):182–193
Feng H, Guo J, Ma X, Han M, Kneeshaw D, Sun H et al (2022) Methane emissions may be driven by hydrogenotrophic methanogens inhabiting the stem tissues of poplar. New Phytol 233:182–193
Ferry B, Morneau F, Bontemps JD, Blanc L, Freycon V (2010) Higher treefall rates on slopes and waterlogged soils result in lower stand biomass and productivity in a tropical rain forest. J Ecol 98:106–116
Fuss R (2020) Gasfluxes: greenhouse gas flux calculation from chamber measurements. R package version 0.4-4. Available online https://cran.r-project.org/web/packages/gasfluxes/gasfluxes.pdf. Accessed 8 Jul 2022
Gauci V, Figueiredo V, Gedney N, Pangala SR, Stauffer T, Weedon GP, Enrich-Prast A (2022) Non-flooded riparian Amazon trees are a regionally significant methane source. Phil Trans R Soc A 380:20200446
Gourlet-Fleury S, Guehl JM, Laroussinie O. (2004). Ecology and management of a neotropical rainforest : lessons drawn from Paracou, a long-term experimental research site in French Guiana. Elsevier, Paris, 336 p. ISBN 2-84299-455-8
Hanson RS, Hanson TE (1996) Methanotrophic bacteria. Microbiol Rev 60:439–471
Hilman B, Angert A (2016) Measuring the ratio of CO_2 efflux to O_2 influx in tree stem respiration. Tree Physiol 36:1422–1431
Janssens IA, Barigah ST, Ceulemans R (1998) Soil CO_2 efflux rates in different tropical vegetation types in French Guiana. Ann Sci For 55:1–10
Jeffrey LC, Reithmaier G, Sippo JZ, Johnston SG, Tait DR, Harada Y, Maher DT (2019) Are methane emissions from mangrove stems a cryptic carbon loss pathway? Insights from a catastrophic forest mortality. New Phytol 224:146–154

Jeffrey LC, Maher DT, Tait DR, Euler S, Johnston SG (2020) Tree stem methane emissions from subtropical lowland forest (Melaleuca quinquenervia) regulated by local and seasonal hydrology. Biogeochemistry 151:273–290

Katayama A, Kume T, Komatsu H, Ohashi M, Matsumoto K, Ichihashi R, ..., Otsuki K (2014) Vertical variations in wood CO_2 efflux for live emergent trees in a Bornean tropical rainforest. Tree Physiol 34: 503-512

Katayama A, Kume T, Ohashi M, Matsumoto K, Nakagawa M, Saito T et al (2016) Characteristics of wood CO_2 efflux in a Bornean tropical rainforest. Agric For Meteorol 220:190–199

Katayama A, Endo I, Makita N, Matsumoto K, Kume T, Ohashi M (2021) Vertical variation in mass and CO_2 efflux of litter from the ground to the 40m high canopy in a Bornean tropical rainforest. Agric For Meteorol 311:108659

Luizão RC, Luizão FJ, Paiva RQ, Monteiro TF, Sousa LS, Kruijt B (2004) Variation of carbon and nitrogen cycling processes along a topographic gradient in a central Amazonian forest. Glob Chang Biol 10:592–600

Machacova K, Papen H, Kreuzwieser J, Rennenberg H (2013) Inundation strongly stimulates nitrous oxide emissions from stems of the upland tree Fagus sylvatica and the riparian tree Alnus glutinosa. Plant Soil 364:287–301

Machacova K, Bäck J, Vanhatalo A, Halmeenmäki E, Kolari P, Mammarella I et al (2016) Pinus sylvestris as a missing source of nitrous oxide and methane in boreal forest. Sci Rep 6:1–8

Machacova K, Vainio E, Urban O, Pihlatie M (2019) Seasonal dynamics of stem N_2O exchange follow the physiological activity of boreal trees. Nat Commun 10:1–13

Machacova K, Borak L, Agyei T, Schindler T, Soosaar K, Mander Ü, Ah-Peng C (2021) Trees as net sinks for methane (CH_4) and nitrous oxide (N_2O) in the lowland tropical rain forest on volcanic Réunion Island. New Phytol 229:1983–1994

Machacova K, Borak L, Agyei T, Schindler T, Soosaar K, Mander Ü, Ah-Peng C (2020) Trees as net sinks for methane (CH4) and nitrous oxide (N2O) in the lowland tropical rain forest on volcanic Réunion Island. New Phytologist 229(4):1983–1994

Maier CA (2001) Stem growth and respiration in loblolly pine plantations differing in soil resource availability. Tree Physiol 21:1183–1193

Maier M, Machacova K, Lang F, Svobodova K, Urban O (2018) Combining soil and tree-stem flux measurements and soil gas profiles to understand CH_4 pathways in Fagus sylvatica forests. J Plant Nutr Soil Sci 181:31–35

Megonigal JP, Guenther AB (2008) Methane emissions from upland forest soils and vegetation. Tree Physiol 28:491–498

Mitchard ET (2018) The tropical forest carbon cycle and climate change. Nature 559:527–534

Moldaschl E, Kitzler B, Machacova K, Schindler T, Schindlbacher A (2021) Stem CH4 and N2O fluxes of Fraxinus excelsior and Populus alba trees along a flooding gradient. Plant and Soil 461:407–420

Paine CET, Stahl C, Courtois EA, Patiño S, Sarmiento C, Baraloto C (2010) Functional explanations for variation in bark thickness in tropical rain forest trees. Funct Ecol 24:1202–1210

Pan Y, Birdsey R, Fang J, Houghton R, Kauppi PE, Kurz W, Phillips OL, Shvidenko A, Lewis SL, Canadell JG, Ciais P, Jackson RB, Pacala SW, McGuire D, Piao S, Rautiainen A, Sitch S, Hayes D (2011) A large and persistent carbon sink in the world's forests. Science 333:988–993

Pangala SR, Moore S, Hornibrook ER, Gauci V (2013) Trees are major conduits for methane egress from tropical forested wetlands. New Phytol 197:524–531

Pangala SR, Enrich-Prast A, Basso LS, Peixoto RB, Bastviken D, Hornibrook ER et al (2017) Large emissions from floodplain trees close the Amazon methane budget. Nature 552:230–234

Parkin TB, Venterea RT, Hargreaves SK (2012) Calculating the detection limits of chamber-based soil greenhouse gas flux measurements. J Environ Qual 41:705–715

Pavelka M, Acosta M, Kiese R, Altimir N, Brümmer C, Crill P et al (2018) Standardisation of chamber technique for CO_2, N_2O and CH_4 fluxes measurements from terrestrial ecosystems. Int Agrophysics 32:569–587

Pedersen AR, Petersen SO, Schelde K (2010) A comprehensive approach to soil-atmosphere trace-gas flux estimation with static chambers. Eur J Soil Sci 61:888–902

Phillips OL, Brienen RJ (2017) Carbon uptake by mature Amazon forests has mitigated Amazon nations' carbon emissions. Carbon Bal Manag 12:1–9

Pitz S, Megonigal JP (2017) Temperate forest methane sink diminished by tree emissions. New Phytol 214:1432–1439

Pitz SL, Megonigal JP, Chang CH, Szlavecz K (2018) Methane fluxes from tree stems and soils along a habitat gradient. Biogeochemistry 137:307–320

Plain C, Ndiaye FK, Bonnaud P, Ranger J, Epron D (2019) Impact of vegetation on the methane budget of a temperate forest. New Phytol 221:1447–1456

R Core Team (2020) R: A language and environment for statistical computing. R Foundation for Statistical Computing, Vienna, Austria. https://www.R-project.org/

Robertson AL, Malhi Y, Farfan-Amezquita F, Aragao LEOC, Silva Espejo JE, Robertson MA (2010) Stem respiration in tropical forests along an elevation gradient in the Amazon and Andes. Glob Chang Biol 16:3193–3204

Roland M, Serrano-Ortiz P, Kowalski AS, Goddéris Y, Sánchez-Cañete EP, Ciais P et al (2013) Atmospheric turbulence triggers pronounced diel pattern in karst carbonate geochemistry. Biogeosciences 10:5009–5017

Rowland L, Hill TC, Stahl C, Siebicke L, Burban B, Zaragoza-Castells J et al (2014) Evidence for strong seasonality in the carbon storage and carbon use efficiency of an Amazonian forest. Glob Chang Biol 20:979–991

Rowland L, da Costa AC, Oliveira AA, Oliveira RS, Bittencourt PL, Costa PB et al (2018) Drought stress and tree size determine stem CO_2 efflux in a tropical forest. New Phytol 218:1393–1405

Ryan MG (1990) Growth and maintenance respiration in stems of *Pinus contorta* and *Picea engelmannii*. Can J For Res 20:48–57

Ryan MG, Waring RH (1992) Maintenance respiration and stand development in a subalpine lodgepole pine forest. Ecology 73:2100–2108

Salomón RL, De Roo L, Bodé S, Boeckx P, Steppe K (2021) Efflux and assimilation of xylem-transported CO_2 in stems

and leaves of tree species with different wood anatomy. Plant Cell Environ 44:3494–3508
Salomón RL, De Roo L, Oleksyn J, Steppe K (2022) Mechanistic drivers of stem respiration: a modelling exercise across species and seasons. Plant Cell Environ 45:1270–1285
Sancho-Knapik D, Mendoza-Herrer Ó, Alonso-Forn D, Saz MÁ, Martín-Sánchez R, dos Santos Silva JV et al (2022) Vapor pressure deficit constrains transpiration and photosynthesis in holm oak: a comparison of three methods during summer drought. Agric For Meteorol 327:109218
Saunois M, Stavert AR, Poulter B, Bousquet P, Canadell JG, Jackson RB et al (2020) The global methane budget 2000–2017. Earth Syst Sci Data 12:1561–1623
Saveyn A, Steppe K, McGuire MA, Lemeur R, Teskey RO (2008) Stem respiration and carbon dioxide efflux of young Populus deltoides trees in relation to temperature and xylem carbon dioxide concentration. Oecologia 154:637–649
Schindler T, Mander Ü, Machacova K, Espenberg M, Krasnov D, Escuer-Gatius J et al (2020) Short-term flooding increases CH_4 and N_2O emissions from trees in a riparian forest soil-stem continuum. Sci Rep 10:1–10
Sjögersten S, Siegenthaler A, Lopez OR, Aplin P, Turner B, Gauci V (2020) Methane emissions from tree stems in neotropical peatlands. New Phytol 225:769–781
Smith KA, Ball T, Conen F, Dobbie KE, Massheder J, Rey A (2003) Exchange of greenhouse gases between soil and atmosphere: interactions of soil physical factors and biological processes. Eur J Soil Sci 54:779–791
Soong JL, Fuchslueger L, Marañon-Jimenez S, Torn MS, Janssens IA, Penuelas J, Richter A (2020) Microbial carbon limitation: the need for integrating microorganisms into our understanding of ecosystem carbon cycling. Glob Chang Biol 26:1953–1961
Sorz J, Hietz P (2006) Gas diffusion through wood: implications for oxygen supply. Trees 20:34–41
Stahl C, Burban B, Goret JY, Bonal D (2011) Seasonal variations in stem CO_2 efflux in the Neotropical rainforest of French Guiana. Ann For Sci 68:771–782
Terazawa K, Yamada K, Ohno Y, Sakata T, Ishizuka S (2015) Spatial and temporal variability in methane emissions from tree stems of Fraxinus mandshurica in a cool-temperate floodplain forest. Biogeochemistry 123:349–362
Teskey RO, Saveyn A, Steppe K, McGuire MA (2008) Origin, fate and significance of CO_2 in tree stems. New Phytol 177:17–32
Teskey RO, McGuire MA, Bloemen J, Aubrey DP, Steppe K (2017) Respiration and CO_2 fluxes in trees. Plant respiration: Metabolic fluxes and carbon balance, 181-207
Townsend AR, Asner GP, Cleveland CC (2008) The biogeochemical heterogeneity of tropical forests. Trends Ecol Evol 23:424–431
Trumbore SE, Angert A, Kunert N, Muhr J, Chambers JQ (2013) What's the flux? Unraveling how CO_2 fluxes from trees reflect underlying physiological processes. New Phytol 197:353–355
Van Langenhove L, Verryckt LT, Stahl C, Courtois EA, Urbina I, Grau O et al (2021) Soil nutrient variation along a shallow catena in Paracou, French Guiana. Soil Res 59:130–145
Wang ZP, Gu Q, Deng FD, Huang JH, Megonigal JP, Yu Q, ..., Han XG (2016) Methane emissions from the trunks of living trees on upland soils. New Phytol 211: 429-439
Warner DL, Villarreal S, McWilliams K, Inamdar S, Vargas R (2017) Carbon dioxide and methane fluxes from tree stems, coarse woody debris, and soils in an upland temperate forest. Ecosystems 20:1205–1216
Welch BWC (2018) Trace Greenhouse Gas Fluxes in Upland Forests. Doctoral dissertation, Open University (United Kingdom)
Welch B, Gauci V, Sayer EJ (2019) Tree stem bases are sources of CH_4 and N_2O in a tropical forest on upland soil during the dry to wet season transition. Glob Chang Biol 25:361–372
Wen Y, Corre MD, Rachow C, Chen L, Veldkamp E (2017) Nitrous oxide emissions from stems of alder, beech and spruce in a temperate forest. Plant Soil 420:423–434
Westerband AC, Wright IJ, Eller AS, Cernusak LA, Reich PB, Perez-Priego O et al (2022) Nitrogen concentration and physical properties are key drivers of woody tissue respiration. Ann Bot 129:633–646
Whitaker J, Ostle N, Nottingham AT, Ccahuana A, Salinas N, Bardgett RD et al (2014) Microbial community composition explains soil respiration responses to changing carbon inputs along an Andes-to-Amazon elevation gradient. J Ecol 102:1058–1071
Wolf K, Flessa H, Veldkamp E (2012) Atmospheric methane uptake by tropical montane forest soils and the contribution of organic layers. Biogeochemistry 111:469–483
Yip DZ, Veach AM, Yang ZK, Cregger MA, Schadt CW (2019) Methanogenic Archaea dominate mature heartwood habitats of Eastern Cottonwood (Populus deltoides). New Phytol 222:115–121
Zhao K, Zheng M, Fahey TJ, Jia Z, Ma L (2018) Vertical gradients and seasonal variations in the stem CO2 efflux of Larix principis-rupprechtii Mayr. Agricultural and Forest Meteorology 262:71–80